

# LLaVA-MoD: MAKING LLaVA TINY VIA MoE-KNOWLEDGE DISTILLATION

Fangxun Shu<sup>1\*</sup> Yue Liao<sup>2,3\*</sup> Le Zhuo<sup>2†</sup> Chenning Xu<sup>1†</sup> Guanghao Zhang<sup>1†</sup>  
 Haonan Shi<sup>1†</sup> Long Chen<sup>1</sup> Tao Zhong<sup>1</sup> Wanggui He<sup>1</sup> Siming Fu<sup>1</sup>  
 Haoyuan Li<sup>1</sup> Bolin Li<sup>1</sup> Zhelun Yu<sup>1</sup> Si Liu<sup>4‡</sup> Hongsheng Li<sup>2,3‡</sup> Hao Jiang<sup>1‡</sup>

<sup>1</sup>Alibaba <sup>2</sup>The Chinese University of Hong Kong

<sup>3</sup>Centre for Perceptual and Interactive Intelligence, Hong Kong <sup>4</sup>Beihang University

## ABSTRACT

We introduce LLaVA-MoD, a novel framework designed to enable the efficient training of small-scale Multimodal Language Models (*s*-MLLM) by distilling knowledge from large-scale MLLM (*l*-MLLM). Our approach tackles two fundamental challenges in MLLM distillation. First, we optimize the network structure of *s*-MLLM by integrating a sparse Mixture of Experts (MoE) architecture into the language model, striking a balance between computational efficiency and model expressiveness. Second, we propose a progressive knowledge transfer strategy to ensure comprehensive knowledge migration. This strategy begins with mimic distillation, where we minimize the Kullback-Leibler (KL) divergence between output distributions to enable the student model to emulate the teacher network’s understanding. Following this, we introduce preference distillation via Direct Preference Optimization (DPO), where the key lies in treating *l*-MLLM as the reference model. During this phase, the *s*-MLLM’s ability to discriminate between superior and inferior examples is significantly enhanced beyond *l*-MLLM, leading to a better student that surpasses its teacher, particularly in hallucination benchmarks. Extensive experiments demonstrate that LLaVA-MoD outperforms existing models across various multimodal benchmarks while maintaining a minimal number of activated parameters and low computational costs. Remarkably, LLaVA-MoD, with only 2B activated parameters, surpasses Qwen-VL-Chat-7B by an average of 8.8% across benchmarks, using merely 0.3% of the training data and 23% trainable parameters. These results underscore LLaVA-MoD’s ability to effectively distill comprehensive knowledge from its teacher model, paving the way for the development of more efficient MLLMs. The code will be available on <https://github.com/shufangxun/LLaVA-MoD>

## 1 INTRODUCTION

Leveraging the advanced instruction-following and reasoning capabilities of Large Language Models (LLMs) (Achiam et al., 2023; Bai et al., 2023a; Jiang et al., 2024; Team et al., 2023; Touvron et al., 2023a;b; Dubey et al., 2024), Multimodal Large Language Models (MLLMs) (Bai et al., 2023b; Liu et al., 2024; Lin et al., 2024b; Li et al., 2023b; Chen et al., 2023b; Shu et al., 2023; Lu et al., 2024), typically integrate a visual encoder (Caron et al., 2021; Radford et al., 2021; Liu et al., 2022) alongside an LLM to achieve promising results across various vision and cross-modal tasks, such as image captioning and visual question-answering. MLLMs are characterized by their large model size and extensive training data, which contribute to their superior performance but also necessitate significant computation resources. For instance, the largest version of LLaVA-NeXT (Li et al., 2024a) employs Qwen-1.5-110B (Yang et al., 2024) as the language model and requires 18 hours of training with 128 H800 GPUs. Furthermore, MLLMs face deployment challenges due to the high memory and computational demands. For instance, models with substantial parameters

\*Equal Contribution

†Core Members

‡Corresponding Authors

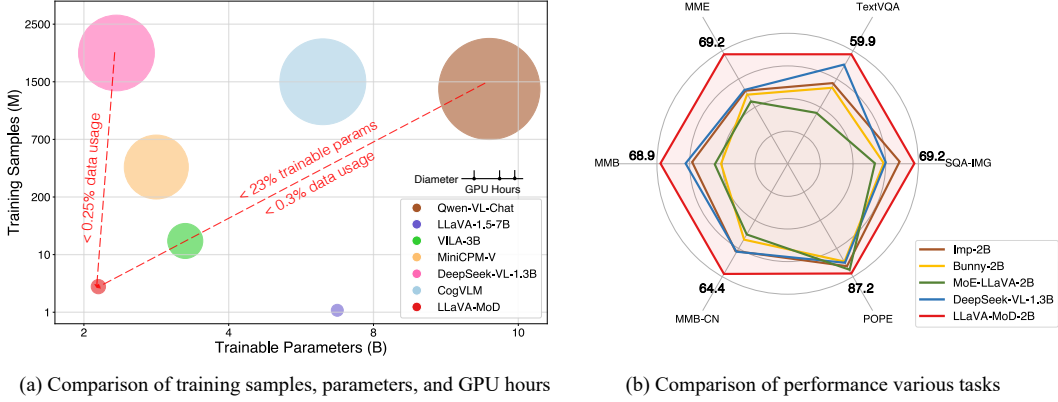


Figure 1: Comparisons of training cost and performance. LLaVA-MoD achieves competitive performance with advanced MLLMs using significantly lower training costs while outperforming current small-scale MLLMs by a large margin.

often require advanced hardware and exhibit slow inference speeds, which significantly hinder their real-world applications such as on mobile devices. Thus, developing MLLMs that balance performance and efficiency has become a crucial research focus.

Previous works on small-scale Multimodal Large Language Models (*s*-MLLM) (Zhou et al., 2024a; Yuan et al., 2023; Shao et al., 2024; He et al., 2024; Chu et al., 2023; 2024; Yao et al., 2024) have mainly concentrated on devising data collection (Schuhmann et al., 2021; 2022; Zhu et al., 2024; Awadalla et al., 2024; Gadre et al., 2024; Chen et al., 2023a) and filtering protocols (Xu et al., 2023; Fan et al., 2024; Zhang et al., 2023; Li et al., 2024b; Nguyen et al., 2024) to ensure high-quality training data. While such high-quality data aid *s*-MLLM in narrowing the performance gap with their larger counterparts, their effectiveness is still limited by model capacity and the availability of high-quality data. With the advent of open-source MLLMs, an intuitive strategy inspired by conventional deep learning tasks involves utilizing large-scale MLLMs (*l*-MLLM) as the teacher to improve the training of *s*-MLLM via Knowledge Distillation (KD) (Hinton et al., 2015). KD facilitates stable and efficient training of smaller models by aligning the output distributions of the student model with those of the teacher model. However, the application of KD as a model reduction technique has yet to be extensively explored in MLLMs. To develop an effective framework for MLLM distillation, we consider two primary challenges. The first challenge lies in designing a lightweight architecture for student MLLMs that retains strong learning and expressive capabilities, enabling it to absorb the complex knowledge embedded within teacher MLLMs effectively. The second challenge is to efficiently and comprehensively transfer this knowledge from the teacher MLLMs to the student MLLMs.

To address these two challenges, we present **LLaVA-MoD**<sup>1</sup>, an effective framework for training *s*-MLLM by mimicking the behavior of the *l*-MLLM through Mixture-of-Expert (MoE) Knowledge Distillation. For the first challenge—designing a lightweight *s*-MLLM structure—a straightforward approach might involve reducing the scale of the base language model in *l*-MLLM to create a smaller network. However, this direct reduction in network parameters can significantly compromise the model’s expressive capability, making it less effective in modeling complex multimodal understanding tasks. Drawing inspiration from the recent success of sparse MoE (Lin et al., 2024a; Dai et al., 2024; Jiang et al., 2024; Shen et al., 2023) in sequential modeling, we incorporate a sparse MoE structure into the dense *s*-MLLM. This approach seeks to balance scale reduction while preserving the model’s ability to capture and represent intricate multimodal information during distillation. Specifically, we enhance the *s*-MLLM by equipping it with several feedforward networks (FFNs) and linear gates within the LLM. Each FFN acts as an expert, capturing fine-grained knowledge from the *l*-MLLM, while the gates select the top-*k* experts to facilitate optimal knowledge transfer pathways.

<sup>1</sup>MoD denotes Mixture-of-Expert Knowledge Distillation for MLLM

To address the second challenge, we propose a progressive distillation strategy for effective knowledge transfer. The process begins by aligning the vision encoder with the LLM using a learnable adapter, thereby initializing a dense student MLLM. Following this, we employ two consecutive distillation stages, where the student model evolves from mimicking and approximating the teacher MLLM to ultimately surpassing it: **Mimic Distillation**. This stage is divided into two steps, *i.e.*, dense-to-dense and dense-to-sparse distillation. In the dense-to-dense distillation stage, we employ standard knowledge distillation loss to align the output logits distribution between the initialized dense  $s$ -MLLM and the teacher model, using general captioning and conversation datasets. Next, we transition to the dense-to-sparse distillation where we transform the dense student MLLM into a sparse one by integrating MoE, and then distill knowledge from the teacher MLLM into this sparse student model using a broad range of tasks and datasets. **Preference Distillation**. In this stage, the teacher model provides knowledge regarding what constitutes “good” and “bad” samples, establishing a foundational reference for the student model. The student MLLM leverages this knowledge to adjust its probability distribution, ensuring that good samples have a higher probability than those from the teacher model, while bad samples are assigned a lower probability. This process enhances the student model’s ability to mitigate hallucinations by improving its judgment capabilities beyond those of the teacher model.

As illustrated in Figure 1, LLaVA-MoD exhibits impressive performance across various multimodal benchmarks while maintaining minimal activated parameters and low computational resources. For example, LLaVA-MoD-2B exceeds Qwen-VL-Chat-7B by an average of 8.8% on these benchmarks, utilizing just 0.3% of the training data and 23% trainable parameters. Furthermore, it matches the performance of RLHF-based methods with 7B and 13B parameters on several hallucination benchmarks. Specifically, LLaVA-MoD-2B surpasses RLHF-V (Yu et al., 2024a) by 8.2% in response-level hallucination rate and by 21.3% in mention-level hallucination rate on the Object HalBench. The impressive results demonstrate the effectiveness of our proposed MoD framework in transferring knowledge from  $l$ -MLLM to  $s$ -MLLM.

## 2 RELATED WORK

**Multimodal Large Language Models.** The emergence of large language models (LLMs) has greatly advanced the field of natural language processing. Connecting visual information to LLM to enhance their understanding of multimodal input is crucial for promoting the unified comprehension of vision and language. CLIP (Radford et al., 2021) was the first to align visual and textual information into a unified embedding space through contrastive learning objectives. BLIP-2 (Li et al., 2023b) utilizes various pre-training tasks to train separate visual and text streams, and adds additional intermediary structures to adapt visual features to LLM. Flamingo (Alayrac et al., 2022) incorporates additional cross-attention modules into LLM to handle arbitrarily interleaved sequences of images and texts. Recently, models like LLaVA (Liu et al., 2024) and MiniGPT-4 (Zhu et al., 2023) use linear projection layers to map image features to the textual space and enhance the models’ instruction-following ability through visual instruction tuning. Moreover, some works focus on a stronger vision encoder. Intern-VL (Chen et al., 2023b) leverages a larger-scale vision encoder to bridge the gap with a large-scale language model, and Mini-Gemini (Li et al., 2024c) introduces additional vision encoders for high-resolution refinement to enhance visual tokens. Qwen-VL (Bai et al., 2023b), VisionLLM (Wang et al., 2023c), and others aim to imbue models with stronger fine-grained visual understanding capabilities, such as grounding and region understanding. Unlike these approaches, our method does not emphasize enlarging the model to boost multimodal capabilities. Instead, we adopt a distillation approach to compress the capabilities of larger models into a smaller, sparse MoE architecture, enhancing computational and storage efficiency.

**Knowledge Distillation.** Large language models possess powerful capabilities, but their enormous size and high inference costs limit their application in low-resource environments. Knowledge distillation (Hinton et al., 2015) uses a large model as teacher to transfer its advanced knowledge to a smaller student model, which plays a critical role in compressing model size and enables smaller models to self-improve. Some works adopt additional designs to make the distillation process more suitable for LLMs. MiniLLM (Gu et al., 2023) minimizes the reverse KLD (Kullback–Leibler divergence) to prevent students from overestimating low-probability regions in the teacher distribution, while GKD (Agarwal et al., 2023) introduces generalized knowledge distillation and promotes the integration of distillation with RLHF (Reinforcement Learning from Human Feedback). Addition-

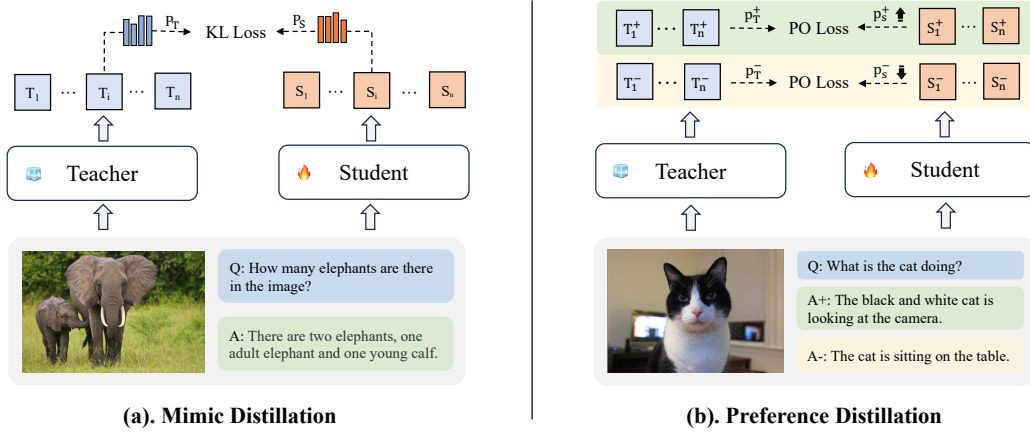


Figure 2: Progressive Distillation of LLaVA-MoD. (a). Mimic Distillation: Aligning the student’s response probabilities  $p_S$  with those of the teacher  $p_T$ , via the Kullback–Leibler (KL) Loss. (b). Preference Distillation: Increasing the student’s positive response probabilities  $p_S^+$  to surpass those of the teacher  $p_T^+$ , while decreasing the student’s negative response probabilities  $p_S^-$  to fall below those of the teacher  $p_T^-$ , via the Preference-Optimization (PO) Loss.

ally, Huang et al. (Huang et al., 2022) introduce context distillation, and some works (Mukherjee et al., 2023; Li et al., 2022; Ho et al., 2023) adopt CoT (Chain-of-Thought) distillation to enhance specific skills of small models. Our approach innovatively distills the knowledge of MLLM into a smaller sparse MoE (Mixture-of-Experts) architecture, significantly enhancing the multimodal processing capabilities of small models at a minimal cost.

**Mixture-of-Experts** The mixture of experts (MoE) architecture is initially introduced by Jacobs et al. (1991) to enhance model performance across various samples through the utilization of independent experts. Recently, with the rise of transformer architectures, numerous studies have extended transformer layers to incorporate MoE. In transformer-based MoE architecture, feed-forward neural network (FFN) layers are often replaced with sparsely activated experts, employing a trainable Top-k gating strategy (Lepikhin et al., 2020; Fedus et al., 2022), thereby effectively increasing model capacity while maintaining a low computational overhead. Additionally, to further mitigate training costs, the sparse upcycling method (Komatsuzaki et al., 2022) is adopted, which initializes expert parameters using those from a well-trained dense model. Currently, MoE architectures have found widespread application not only in pre-trained language models (Jiang et al., 2024; Dai et al., 2024) but also in vision models and vision-language models (Lin et al., 2024a; Shen et al., 2023). Our approach integrates MoE with knowledge distillation techniques to provide stronger signals for sparse training, which remarkably decrease the training cost associated with sparse models.

### 3 METHOD

We introduce LLaVA-MoD, a novel framework for building efficient MLLM using mixture-of-experts (MoE) knowledge distillation. Our framework consists of two main components: (a). *Architecture Design of s-MLLM*: As shown in Figure 3, we design the s-MLLM with a sparse MoE framework, enhancing the ability to acquire specialized expert knowledge. (b). *Distillation Mechanism*: We design a progressive distillation mechanism as shown in Figure 2 to transfer knowledge from the l-MLLM to the sparse s-MLLM. This process involves two stages: mimic distillation followed by preference distillation. We will introduce LLaVA-MoD in detail from these two components.

#### 3.1 ARCHITECTURE DESIGN OF SPARSE s-MLLM

In this section, we describe the architecture design of our sparse s-MLLM, which serves as the student model in the distillation process.

**$s$ -MLLM Definition.** As illustrated in Figure 3, the basic architecture of  $s$ -MLLM consists of three primary components: a vision encoder, a large language model (LLM), and a vision-language (VL) adaptor. Given a multimodal instruction conversation  $(x, y)$ , we define our  $s$ -MLLM to process response  $y$  as follows:

$$y = \text{LLM}_\phi(\text{Proj}_\omega(\text{ViT}_\chi(x_v)), x_i), \quad (1)$$

where  $x_v$  is the input image, and  $x_i$  is the text instruction. The input image is resized to  $336 \times 336$  and patched into 576 image tokens, each of size  $14 \times 14$ .  $\text{ViT}_\chi$  is the CLIP vision encoder with parameters  $\chi$  which first extracts image features from  $x_v$ .  $\text{Proj}_\omega$  is the vision-language adaptor with parameters  $\omega$ , serving as the vision tokenizer to align the image features with the word embedding space.  $\text{LLM}_\phi$  is the large language model with parameters  $\phi$ , which produces the response  $y$  based on the multimodal tokens of  $x = [x_v, x_i]$ .

**Mixture-of-Experts.** The principle of building our  $s$ -MLLM is downsizing the LLM while leaving the vision encoder and vision-language adaptor unmodified. To achieve this downsizing goal, we sparsify the dense  $s$ -MLLM by incorporating an MoE architecture. Specifically, Figure 3 illustrates the process, where we apply the sparse upcycling technique (Komatsuzaki et al., 2022) to replicate  $N$  feedforward networks (FFNs) as the expert modules. Additionally, we introduce a linear layer as the router, which dynamically activates the appropriate experts by predicting the probability of expert assignment. Given each token  $x$  in the sequence, we first compute the routing value of  $N$  experts:

$$r = \text{Softmax}(x \cdot W_r), \quad (2)$$

where  $W_r$  denotes the weight matrix of the router and each element  $r_i$  in  $r$  represents the probability of activating the  $i$ -th expert. After that, we apply the Top- $k$  strategy to determine the activated experts with the highest  $k$  routing values:

$$\tilde{r} = \text{Top-}k(r) = \begin{cases} r_i, & \text{if } i \in k \\ 0, & \text{otherwise} \end{cases} \quad (3)$$

where the routing values for the inactivated experts are set to zero, effectively excluding them from contributing to the final output. The output  $y$  is calculated by aggregating the contributions of the activated experts, weighted by their corresponding routing values:

$$y = \sum_{i=1}^N \tilde{r} \cdot E_i(x). \quad (4)$$

### 3.2 PROGRESSIVE DISTILLATION

Our progressive distillation consists of two distinct stages, *i.e.*, mimic distillation (Figure 2 (a)) and preference distillation (Figure 2 (b)). In the mimic distillation stage, the student MLLM  $\pi_S$  imitates the general and specific knowledge from the teacher MLLM  $\pi_T$ . In the preference distillation stage, the student MLLM gains the preference knowledge of the teacher MLLM to further refine its output and reduce hallucinations. We use the pre-trained  $l$ -MLLM as the teacher MLLM, which is frozen during the whole distillation process. Both teacher and student MLLMs are in the same LLM family, ensuring consistent vocabulary space, which is essential for the student MLLM to imitate the teacher MLLM accurately. For simplicity, we denote the student as  $\pi_S$  and the teacher as  $\pi_T$ .

**Initialization.** Before distillation, we first align the vision encoder with the LLM via a learnable adapter, aiming to obtain a well-initialized dense student MLLM. The  $\text{LLM}_\phi$  and  $\text{ViT}_\chi$  are maintained frozen since their pre-trained parameters have already captured rich visual and language knowledge. Only  $\text{Proj}_\omega$  is optimized to bridge the gap between the vision and language domain. For

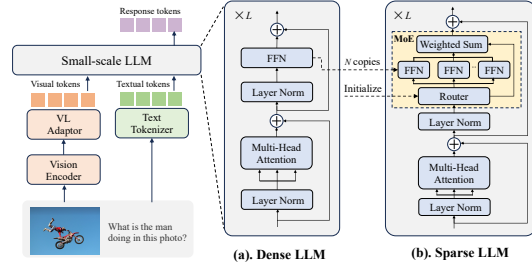


Figure 3: Dense to Sparse Architecture of LLaVA-MoD. The architecture of LLaVA-MoD consists of three components: VL Adaptor, Vision Encoder, and LLM. The VL Adaptor and Vision Encoder remain unchanged, while the LLM is up-cycled from dense to sparse.

the initialization, we utilize common image-caption pairs from a widely used and curated dataset, which covers a diverse range of subjects and visual entities. The training objective is to minimize the cross-entropy of the generated tokens. The objective function is defined as:

$$\mathcal{L}_{\text{Init}}(\pi_S) = -\mathbb{E}_{(y_k | y_{<k}, x) \sim \pi_S} [\log \pi_S(y_k | y_{<k}, x)], \quad (5)$$

where  $\pi_S(y_k | y_{<k}, x)$  represents the probability of the predicted token  $y_k$  conditioned on  $x$  and the previous tokens  $y_{<k} = (y_1, y_2, \dots, y_{k-1})$ .

**Mimic Distillation.** We decompose the comprehensive knowledge of the teacher MLLM into general and expertise aspects and undertake dense-to-dense distillation and dense-to-sparse distillation respectively to transfer this knowledge to the student MLLM.

**a). Dense-to-Dense Distillation.** In this stage, we aim to replicate the general knowledge of the teacher MLLM. Acquiring general knowledge first is crucial, as it provides a broad foundation and common understanding across various domains, enabling the student MLLM to develop a basic framework applicable in multiple scenarios. This foundation supports a more comprehensive and flexible understanding before progressing to specialized tasks. To achieve this, we maintain ViT <sub>$\chi$</sub>  frozen, and jointly optimize LLM <sub>$\phi$</sub>  and Proj <sub>$\omega$</sub> , with trainable parameters  $\theta = \{\omega, \phi\}$ . We leverage common image-caption pairs and conversation datasets. The training objective is to minimize the Kullback-Leibler divergence (KLD) between the output logits of the dense student MLLM and the teacher MLLM. The objective function is defined as:

$$\mathcal{L}_{\text{D2D}}(\pi_S; \pi_T) = -\mathbb{E}_{(x, y_k) \sim \pi_T} \left[ \log \frac{\pi_T(y_k | y_{<k}, x)}{\pi_S(y_k | y_{<k}, x)} \right], \quad (6)$$

where  $V$  denotes the vocabulary, while  $\pi_S(y_k | y_{<k}, x)$  and  $\pi_T(y_k | y_{<k}, x)$  denote the probability of the predicted tokens for student and teacher models, respectively.

**b). Dense-to-Sparse Distillation.** In this stage, our focus shifts to transferring the specialized expertise of the teacher MLLM, allowing the student MLLM to obtain advanced capabilities and achieve superior performance in diverse tasks. However, directly learning this knowledge in its dense form could lead to inefficiencies and difficulty. Therefore, we sparsify the dense student MLLM by introducing multiple experts. As detailed in Section 3.1, we replicate  $N$  feedforward networks (FFNs) within LLM <sub>$\phi$</sub>  and incorporate an MLP layer as a router, which jointly constitutes the experts with parameters  $\phi_e$ . This sparse architecture allows the student MLLM to selectively activate the most relevant experts for different tasks and inputs, offering significant advantages in emulating the teacher’s specialized knowledge. For training, we leverage multi-task data, updating only the experts and the adaptor. We employ a Top- $k$  routing strategy to select the experts. The trainable parameters are  $\theta = \{\omega, \phi_e\}$ . Similar to the previous stage, we also adopt the KLD as the training objective. Additionally, we include the standard next-token prediction objective, *i.e.*, minimizing the student-generated tokens’ cross-entropy loss, to inject supervision from ground truth data which can reduce the existing bias in the teacher model. The final objective function is defined as:

$$\mathcal{L}_{\text{D2S}}(\pi_S; \pi_T) = -\mathbb{E}_{(x, y_k) \sim \pi_S} [\log \pi_S(y_k | y_{<k}, x)] - \mathbb{E}_{(x, y_k) \sim \pi_T} \left[ \log \frac{\pi_T(y_k | y_{<k}, x)}{\pi_S(y_k | y_{<k}, x)} \right]. \quad (7)$$

**Preference Distillation.** In this stage, our goal is to distill the preference knowledge from the teacher MLLM to guide the student MLLM towards generating not only accurate but also reasonable responses, which is crucial in reducing hallucinations. For the training process, we make effective use of preference data, which comprises meticulously paired positive responses  $y^+$  and negative responses  $y^-$  for the identical prompt  $x$ . Our preference distillation strategy is inspired by recent advancements in Direct Preference Optimization (DPO) (Rafailov et al., 2024), which bypasses the need for training a reward model by directly training on an offline preference dataset. Our key insight is to treat the teacher MLLM as the reference model during distillation. The teacher model plays a crucial role by providing insights into what constitutes “good” and “bad”, thereby establishing a fundamental reference for the student model.

Specifically, the training objective is to optimize the student model to assign higher probabilities to positive responses than those of the teacher model while assigning lower probabilities to negative responses than those of the teacher model. This training process involves two key optimization aspects: First, the student model seeks to align with the teacher model in distinguishing positive

from negative responses. Second, the student model aims to surpass the teacher model by assigning higher probabilities to positive responses and lower probabilities to negative responses. We only train the mixture of experts and the VL adaptor in the student model and employ a Top- $k$  routing strategy to select the experts. The trainable parameters are  $\theta = \{\omega, \phi_e\}$ . The object function is defined as:

$$\mathcal{L}_{\text{PD}}(\pi_S; \pi_T) = -\mathbb{E}_{(x, y^+, y^-) \sim \mathcal{D}} \left[ \log \sigma \left( \beta \log \frac{\pi_S(y^+ | x)}{\pi_T(y^+ | x)} - \beta \log \frac{\pi_S(y^- | x)}{\pi_T(y^- | x)} \right) \right], \quad (8)$$

where  $\pi_S(y^+ | x)$  and  $\pi_S(y^- | x)$  denote the probabilities of positive and negative responses for the student model, respectively, and  $\pi_T(y^+ | x)$  and  $\pi_T(y^- | x)$  denote the same for the teacher model.

## 4 EXPERIMENTS

### 4.1 EXPERIMENTAL SETTINGS

**Implementation Details.** We employ the well-established "ViT-MLP-LLM" architecture to demonstrate the effectiveness of LLaVA-MoD. Specifically, a pre-trained CLIP-ViT-L/14 is utilized as the vision encoder and a 2-layer MLP is utilized as the adaptor for both the student and the teacher models. Both teacher and student models leverage the Qwen-1.5 and Qwen-2 families to construct their base model. Specifically, the teacher model employs a 7B parameter configuration, while the student model is constructed with 1.8B and 0.5B parameter sizes. The performance of teacher MLLM on common multimodal benchmarks is presented in Table 1.

Table 1: Performance of teacher MLLM on multimodal benchmarks.

LLM	VisEnc	GQA	VisWiz	SQA <sup>I</sup>	VQA <sup>T</sup>	MME	MMB	MMB <sup>CN</sup>	AVG
Qwen-1.5-7B	CLIP-L	62.3	40.7	70.9	55.3	72.1	68.5	64.9	62.1
Qwen-2-7B	CLIP-L	62.5	37.9	73.2	57.2	78.0	71.6	71.1	64.5

As introduced in Section 3.2, the training process comprises mimic distillation and preference distillation, each with specific settings. At initialization, we first freeze the vision encoder and LLM while optimizing the VL adaptor to align image tokens with the word embedding space. This stage employs a cross-entropy loss with a batch size of 512 and a learning rate of 1e-4. In the mimic distillation stage, the vision encoder remains frozen, while the LLM and VL adaptor are co-optimized to distill general knowledge from the teacher MLLM in a dense-to-dense fashion. Then, the FFN in the LLM is first transformed into a sparse architecture with a mixture of FFN experts co-optimized with the VL adaptor to distill specialized knowledge from the teacher MLLM in a dense-to-sparse fashion. This stage employs a KL-divergence loss, with cross-entropy loss added for dense-to-sparse distillation. The batch size is 256, and the learning rate is adjusted to 2e-5. In the preference distillation stage, the model inherits from the mimic distillation. The vision encoder remains frozen, and a mixture of FFN experts is co-optimized with the VL adaptor to distill preference knowledge from the teacher MLLM. This stage employs a DPO loss to optimize the student’s probability for positive responses to be greater than that of the teacher and the student’s probability for negative responses to be lower than that of the teacher. The batch size is 256, and the learning rate is adjusted to 2e-6. Throughout all stages, we employ the adam optimizer (Diederik, 2014) and train on 16 NVIDIA A100 GPUs for one epoch each, totaling approximately 960 GPU hours. The detailed hyperparameters of each training stage are illustrated in Appendix A.2.

**Training Datasets.** The training data consists of 5M samples from the open-source datasets, with each training stage utilizing a distinct dataset. During Initialization, 0.6M general captioning samples from LLaVA-1.5-pretrain dataset (Liu et al., 2023b) are used to bridge the gap between visual and language modalities. In mimic distillation, 2.4M general captioning and conversation samples are used to distill general knowledge from the teacher MLLM and 1.4M multi-tasks data, including VQA, documents, science, and OCR, are used to distill specialized knowledge from the

teacher MLLM. For preference distillation, 0.8M preference data samples are used to transfer preference knowledge from the teacher. The detailed dataset of each training stage is illustrated in Appendix A.1.

**Evaluation Benchmarks.** We conduct experiments on MME (Fu et al., 2023), MMB (Liu et al., 2023c), and MMB<sup>CN</sup>. Each of these encompasses various sub-tasks, enabling comprehensive evaluation of multimodal understanding and reasoning capabilities. Additionally, we carry out experiments across a broad spectrum of VQA tasks, which include general VQA, text-oriented VQA, and science VQA. Specifically, for general VQA tasks, we use VizWiz (Gurari et al., 2018) and GQA (Hudson & Manning, 2019) to test general visual understanding and relational reasoning. TextVQA (Singh et al., 2019) is employed for text-oriented VQA tasks, focusing on fine-grained visual recognition and understanding of text within images. ScienceQA (Lu et al., 2022b) is utilized to measure scientific knowledge. Moreover, we conduct experiments on several hallucination benchmarks such as POPE (Li et al., 2023c), Object HalBench (Yu et al., 2024a), MMHal-Bench (Sun et al., 2023), and AMBER (Wang et al., 2023b).

## 4.2 MAIN RESULTS

In this section, we conduct experiments of LLaVA-MoD to highlight its advantages in two aspects: performance and efficiency. For performance, we evaluate comprehension-oriented benchmarks (Table 2) and hallucination-oriented benchmarks (Table 3). For efficiency, we present a comparison in terms of data samples and model size.

Table 2: Comparison with state-of-the-art MLLMs on the commonly-used multimodal benchmarks for MLLMs. #Sample: Training data sample. #Param: Trainable parameters. SQA<sup>1</sup>: ScienceQA test, VQA<sup>T</sup>: TextVQA val, MME: MME Benchmark, normalized to percentage, MMB: MMBench dev, MMB<sup>CN</sup>: MMBench-Chinese dev. The best result for model sizes 1B/2B is shown in bold, and the second-best result is underlined. Our LLaVA-MoD achieves the best average result for both.

Method	LLM	#Sample	#Param	GQA	VisWiz	SQA <sup>1</sup>	VQA <sup>T</sup>	MME	MMB	MMB <sup>CN</sup>	AVG
BLIP-2	Vicuna-13B	129M	$\geq 7B$	41.0	19.6	61.0	42.5	64.7	-	-	-
VILA-7B	LLaMA-7B	50M		62.3	57.8	68.2	64.4	76.7	68.9	61.7	65.7
CogVLM	Vicuna-7B	1500M		64.9	-	65.6	78.2	71.8	63.7	53.8	-
InstructBLIP	Vicuna-13B	130M		49.5	33.4	63.1	50.7	60.6	-	-	-
IDEFICS-80B	LLaMA-65B	6.8M		38.4	35.5	59.9	25.9	64.2	48.2	25.2	42.5
Qwen-VL-Chat	Qwen-7B	1450M		57.5	38.9	68.2	61.5	74.4	60.6	56.7	56.7
SPHINX-Intern2	InternLM2-7B	15M		56.2	49.6	70.4	58.1	63.2	57.9	-	-
Deepseek-VL-7B	DLLM-7B	2000M		61.3	49.9	74.0	64.7	73.4	74.1	72.8	67.2
LLaVA-1.5-7B	Vicuna-1.5-7B	1.2M		62.0	50.0	66.8	58.2	75.5	64.3	58.3	62.1
LLaVA-NeXT	Vicuna-1.5-13B	1.3M		65.4	60.5	73.6	67.1	78.7	70.0	64.4	68.5
Imp-3B	Phi-2-2.7B	1.6M	$\sim 3B$	63.5	54.1	72.8	59.8	72.3	72.9	46.7	63.2
Bunny-3B	Phi-2-2.7B	2.7M		62.5	43.8	70.9	56.7	74.4	68.6	37.2	59.2
VILA-3B	LLaMA-2.7B	51M		61.5	53.5	69.0	60.4	72.1	63.4	52.7	61.8
LLaVA-Phi	Phi-2-2.7B	1.3M		-	35.9	68.4	48.6	66.7	59.8	-	-
TinyLLaVA	Phi-2-2.7B	3.2M		61.0	-	70.1	53.5	71.6	68.3	-	-
TinyGPT-V	Phi-2-2.7B	24M		33.6	33.4	-	-	-	-	-	-
MobileVLM	MLLaMA-2.7B	1.3M		59.0	-	61.0	47.5	64.4	59.6	-	-
MobileVLM <sup>v2</sup>	MLLaMA-2.7B	3.6M		61.1	-	70.0	57.5	72.0	63.2	-	-
MoE-LLaVA-3B	Phi-2-2.7B	2.2M		61.4	43.9	68.5	51.4	71.1	65.2	41.8	57.6
MiniCPM-V	MiniCPM-2.4B	570M		51.5	50.5	74.4	56.6	68.9	64.0	62.7	61.2
MiniCPM-V-2	MiniCPM-2.4B	570M		52.1	60.2	76.3	73.2	70.5	68.5	67.2	66.9
Imp-2B	Qwen-1.5-1.8B	1.6M	$\sim 2B$	<b>61.9</b>	39.6	66.1	54.5	65.2	63.8	61.2	58.9
Bunny-2B	Qwen-1.5-1.8B	2.7M		59.6	34.2	64.6	53.2	65.0	59.1	58.5	56.3
Mini-Gemini-2B	Gemma-2B	2.7M		60.7	<b>41.5</b>	63.1	56.2	67.0	59.8	51.3	57.1
MoE-LLaVA-2B	Qwen-1.5-1.8B	2.2M		<u>61.5</u>	32.6	63.1	48.0	64.6	59.7	57.3	55.3
DeepSeek-VL-1.3B	DLLM-1.3B	2000M		59.3	36.8	64.2	58.4	65.3	64.6	61.0	58.5
LLaVA-MoD-2B	Qwen-1.5-1.8B	5M		58.7	39.2	68.0	<u>58.5</u>	<u>66.7</u>	<u>66.3</u>	<u>61.9</u>	<u>59.9</u>
LLaVA-MoD-2B	Qwen-2-1.5B	5M		58.8	<u>40.4</u>	<b>69.2</b>	<b>59.9</b>	<b>69.2</b>	<b>68.9</b>	<b>64.4</b>	<b>61.6</b>
SPHINX-Tiny	TLLaMA-1.1B	15M		<b>58.0</b>	<b>49.2</b>	21.5	<b>57.8</b>	63.1	56.6	37.8	49.2
LLaVA-MoD-1B	Qwen-1.5-0.5B	5M	$\sim 1B$	56.2	31.6	<b>62.8</b>	53.9	<u>65.3</u>	<b>58.8</b>	50.4	<u>54.1</u>
LLaVA-MoD-1B	Qwen-2-0.5B	5M		<u>56.6</u>	<u>35.1</u>	<u>61.1</u>	<u>57.1</u>	<b>67.0</b>	<u>58.7</u>	<b>54.1</b>	<b>55.7</b>



#### 4.2.1 COMPREHENSION-ORIENTED BENCHMARKS

As indicated in Table 2, LLaVA-MoD demonstrates remarkable performance on comprehension-oriented benchmarks. It achieves SOTA average results among the models of 2B size and 1B size. Specifically, The 2B-sized LLaVA-MoD surpasses Mini-Gemini-2B (Li et al., 2024c) by 8.1%, while using a lower image resolution (336 vs. 768). The 1B-sized LLaVA-MoD surpasses SPHINX-Tiny (Gao et al., 2024) by 13.2%, using fewer data samples (5M vs. 15M). Furthermore, LLaVA-MoD-2B matches and even surpasses the performance of large-scale MLLMs. Specifically, The 2B-sized LLaVA-MoD surpasses Qwen-VL-Chat-7B (Bai et al., 2023b) by 8.8% and matches the performance of VILA-3B (Lin et al., 2024b) and MiniCPM-V (Yao et al., 2024). These results highlight that our approach effectively and efficiently training small-scale MLLMs by distilling the sparse MoE architecture.

Table 3: Comparison with state-of-the-art MLLMs on the hallucination benchmarks. We compare LLaVA-MoD with SFT-based works and RLHF-based works. Hall: Hallucination Rate Resp: response-level hallucination rate, Ment: mention-level hallucination rate. The best result is in bold, and the second-best result is underlined.

Model	LLM	#Param	Object HalBench		POPE	MMHal Bench	
			Resp ↓	Ment ↓	F1 ↑	Score ↑	Hall ↓
Teacher MLLM	Qwen-1.5-7B	7B	50.1	24.8	84.9	2.60	20.7
Teacher MLLM	Qwen-2-7B	7B	29.7	23.4	85.7	2.88	14.5
Qwen-VL-Chat	Qwen-7B	9.6B	40.4	20.7	74.9	2.76	38.5
LLaVA-1.5-7B	Vicuna-7B	7B	53.6	25.2	86.1	2.36	51.0
VCD	Vicuna-1.5-7B	7B	48.8	24.3	84.5	2.12	54.2
OPERA	Vicuna-1.5-7B	7B	45.1	22.3	85.4	2.15	54.2
HA-DPO	Vicuna-1.5-7B	7B	39.9	19.9	86.8	1.98	60.4
POVID	Vicuna-1.5-7B	7B	48.1	24.4	86.3	2.08	56.2
LLaVA-RLHF	Vicuna-1.5-13B	13B	38.1	18.9	82.7	2.02	62.5
LURE	Vicuna-1.5-7B	7B	27.7	17.3	-	1.64	60.4
RLHF-V	Vicuna-13B	13B	12.2	7.5	86.2	2.45	51.0
RLAIF-V	Vicuna-1.5-7B	7B	8.5	4.3	-	3.06	29.2
MiniCPM-V	MiniCPM-2.4B	2.8B	21.6	11.5	79.5	<u>3.70</u>	24.9
MiniCPM-V-2	MiniCPM-2.4B	2.8B	14.5	7.8	86.3	<b>4.09</b>	18.2
Mini-Gemini-2B	Gemma-2B	2B	29.7	21.1	85.6	2.83	18.8
Bunny-2B	Qwen-1.5-1.8	2.2B	50.2	23.4	85.8	2.72	19.3
LLaVA-MoD-2B	Qwen-1.5-1.8B	2.2B	<u>11.4</u>	<u>7.2</u>	<u>87.0</u>	2.76	<u>17.2</u>
LLaVA-MoD-2B	Qwen-2-1.5B	1.9B	<b>11.2</b>	<b>5.9</b>	<b>87.2</b>	2.91	<b>13.8</b>

#### 4.2.2 HALLUCINATION-ORIENTED BENCHMARKS

As indicated in Table 3, LLaVA-MoD shows remarkable performance in mitigating hallucination, even beating its teacher model. It can be attributed into two aspects: Firstly, by assigning a higher probability for the positive response, preference distillation encourages the student model to focus on providing correct and relevant information. Secondly, by assigning a lower probability for the negative response, preference distillation discourages incorrect or unsubstantiated information. Using the teacher model as a reference to adjust response probabilities, this optimization enables the student model to handle hallucination problems more accurately and reliably, thereby outperforming the teacher model.

Moreover, LLaVA-MoD surpasses similar small-sized models (Yao et al., 2024; Li et al., 2024c; He et al., 2024) and even recent RLHF-based models (Sun et al., 2023; Zhou et al., 2024b; Huang et al., 2024; Leng et al., 2024; Zhou et al., 2023; Zhao et al., 2023b). For instance, on the Object HalBench, it outperforms RLHF-V (Yu et al., 2024a) by 8.2% in response-level hallucination rate and by 21.3% in mention-level hallucination rate. This demonstrates that taking the teacher model as a reference for preference distillation is a challenging task that can encourage the student model to effectively learn to mitigate hallucination.

#### 4.2.3 EFFICIENCY COMPARISON

We compare the efficiency of LLaVA-MoD with recent SOTA MLLMs in terms of training data and trainable parameters. As indicated in Table 2, The 2B-sized LLaVA-MoD requires only 5M samples and activates merely a subset of its total 2.2B parameters during training and inference. It demonstrates that LLaVA-MoD achieves 8.8% higher performance than Qwen-VL-Chat, using only 23% trainable parameters and 0.3% of training data samples, respectively. Moreover, when compared to the small-sized model MiniCPM-V with 2.8B trainable parameters, LLaVA-MoD also achieves superior performance with just 1.6% of the data samples and 2B parameters, underscoring its efficiency. In conclusion, LLaVA-MoD enables more efficient utilization of data, parameters, and computational resources. This not only results in faster training and inference but also provides a practical solution for deploying high-performance models in resource-constrained environments.

#### 4.3 ABLATION STUDY

In this section, we begin by analyzing the impact of preference distillation. Next, we conduct ablation studies on a model trained solely with mimic distillation to investigate the effectiveness of our proposed architecture and training strategy on comprehension-oriented benchmarks. We utilize CLIP-ViT-L/14 as the default vision encoder. The default large language models (LLMs) are Qwen-1.5-1.8B and Qwen-1.5-7B for the student and teacher models.

##### 4.3.1 IMPACT OF PREFERENCE DISTILLATION

We extensively evaluated preference distillation, examining its impact on both the comprehension ability and hallucination mitigation capabilities of LLaVA-MoD. As detailed in Table 4 and Table 5, preference distillation does not yield consistent improvements in comprehension across all benchmarks, its impact on hallucination mitigation was strikingly consistent. Across all evaluated benchmarks, preference distillation notably reduced the occurrence of hallucinations, highlighting its efficacy in enhancing the reliability and factual accuracy of LLaVA-MoD. This observation aligns with the field of language modeling (Achiam et al., 2023), have consistently indicated that RLHF techniques tend to prioritize the reduction of hallucinations, often at the expense of potential gains in other areas, such as raw comprehension scores.

Table 4: Performance of preference distillation on comprehension-oriented benchmarks.

Distillation Stage	GQA	VizWiz	SQA <sup>I</sup>	VQA <sup>T</sup>	MME	MMB	MMB <sup>CN</sup>	AVG
Mimic	59.3	40.0	68.4	58.7	68.4	65.1	61.5	60.2
Mimic + Preference	58.7	39.2	68.0	58.5	66.7	66.3	61.9	59.9

Table 5: Performance of preference distillation on hallucination-oriented benchmarks.

Distillation Stage	Object HalBench		POPE	MMHal Bench	
	Resp ↓	Ment ↓	F1 ↑	Score ↑	Hall ↓
Mimic	39.1	22.6	86.7	2.75	17.8
Mimic + Preference	11.4	7.2	87.0	2.76	17.2

##### 4.3.2 IMPACT OF TRAINING STRATEGY

**Knowledge Distillation Improves Training Efficiency in MoE.** This study explores the impact of knowledge distillation (KD) and examines how it facilitates MoE model training compared to supervised fine-tuning (SFT). The experiments are conducted using the same sparse configuration of E4T2, where 4 experts are initialized and the top-2 experts are activated. The same datasets and training hyperparameters are employed for both KD and SFT.

Training MoE models is inherently challenging, as it requires effectively leveraging huge data to optimize experts’ routing. Our approach demonstrates that KD, compared to traditional SFT, excels in addressing this challenge, achieving superior performance across multiple benchmarks. As demonstrated in Table 6, KD significantly outperforms SFT on all the benchmarks. Specifically, KD achieves an average improvement of 8.1% over SFT, with particularly pronounced gains in complex multi-task scenarios. For instance, on the MMB and MME benchmarks, KD surpasses SFT by 8.2% and 10.0%, respectively. These results highlight KD’s ability to effectively leverage multiple experts and extract comprehensive knowledge from large-scale MLLMs. By distilling essential knowledge, KD not only maximizes data utilization but also achieves better generalization ability of MoE compared to SFT.

Table 6: Comparison between the KD and SFT. The architecture of the student model is configured as E4T2.

Training	GQA	VizWiz	SQA <sup>I</sup>	VQA <sup>T</sup>	MME	MMB	MMB <sup>CN</sup>	AVG
SFT	58.6	31.2	66.2	55.6	63.2	59.2	56.1	55.7
KD	59.3	40.0	68.4	58.7	68.4	65.1	61.5	60.2

**Focusing on Response Improves Distillation Generalization.** This study explores the impact of the distillation target. The default approach distills response, we experiment with distilling both response and instruction. Both settings utilize the same datasets and training hyperparameters. Table 7 shows that distilling only the response achieves superior performance, surpassing jointly distilling response and instruction by 3.1% in terms of average performance. This suggests that focusing on response is more effective for knowledge distillation in auto-regressive modeling. A possible explanation lies in that mimicking instructions could lead to overfitting the specific instruction patterns of training data, potentially reducing the model’s adaptability to unseen instructions. Mimicking the teacher model’s response proves to be effective in improving the student’s auto-regressive modeling generalization capabilities.

Table 7: Comparison between different distillation tokens. The response indicates distilling solely on the generated response tokens, while the response+instruction incorporates additional instruction tokens in the distillation process.

Distillation Tokens	GQA	VizWiz	SQA <sup>I</sup>	VQA <sup>T</sup>	MME	MMB	MMB <sup>CN</sup>	AVG
Response + Instruction	58.5	35.0	66.8	58.3	68.5	61.8	59.0	58.4
Response	59.3	40.0	68.4	58.7	68.4	65.1	61.5	60.2

#### 4.3.3 IMPACT OF MODEL ARCHITECTURE

**Sparse MoE Enables Effective Knowledge Distillation.** This study explores the effect of sparse architecture in distillation by comparing its performance to dense architecture. We adopt the E4T1 configuration as the sparse architecture to ensure the same activated parameters as the dense architecture. The same datasets and training hyperparameters are used for sparse and dense architectures.

Table 8 demonstrates that a sparse Mixture-of-Experts (MoE) architecture significantly outperforms the dense architecture across various benchmarks, achieving an average improvement of 3.7%. This superior performance is particularly evident in complex multi-task settings, such as MME, MMB, and MMB<sup>CN</sup>, where the sparse architecture effectively leverages multiple experts to distill diverse knowledge from the *l*-MLLM. This effectiveness stems from the sparse MoE’s ability to activate only a subset of experts for each input, allowing it to learn specialized knowledge for different tasks. This selective activation significantly reduces computational overhead while maintaining comparable computational efficiency to dense counterparts. As a result, the student model effectively learns from the teacher without introducing excessive computational costs.

Table 8: Comparison between sparse and dense architecture within the distillation. The sparse architecture is configured as E4T1.

Architecture	GQA	VizWiz	SQA <sup>I</sup>	VQA <sup>T</sup>	MME	MMB	MMB <sup>CN</sup>	AVG
Dense	57.6	32.7	67.3	56.8	65.2	61.8	58.2	57.1
Sparse	58.7	36.9	67.9	58.2	66.1	64.5	61.7	59.2

**Teacher Capacity Matters in Knowledge Distillation.** This study explores the impact of the teacher in the distillation process. Specifically, we utilize CLIP-ViT-L/14 as the vision encoder. For the LLM, Qwen-1.5-7B is the strong teacher while Qwen-1.5-4B is the weaker teacher. All experiments are conducted under the same datasets and training hyperparameters to ensure a fair comparison.

As shown in Table 9, a suitable teacher enhances performance across various benchmarks. For instance, the Qwen-1.5-1.8B student model achieves an average performance of 62.3% with the weaker Qwen-1.5-4B teacher. This performance jumps to 63.6% when utilizing the stronger Qwen-1.5-7B teacher. Interestingly, the smaller Qwen-1.5-0.5B student model shows marginal improvement with either the Qwen-1.5-4B or Qwen-1.5-7B teacher. This suggests that an excessively large capacity gap between the teacher and student models can hinder effective knowledge transfer. Utilizing a "middle teacher" with an intermediate capacity could bridge this gap, facilitating smoother knowledge transfer and boosting the student model’s learning efficiency.

Table 9: Comparison between the strong and weak teachers within the distillation. We set the strong teacher as the LLM is Qwen-1.5-7B and the weak teacher as the LLM is Qwen-1.5-4B. The model configuration is E4T2.

Student	Teacher	GQA	VizWiz	SQA <sup>I</sup>	VQA <sup>T</sup>	MME	MMB	MMB <sup>CN</sup>	AVG
Qwen-1.5-0.5B	Qwen-1.5-4B	56.0	25.3	64.7	53.8	63.3	62.2	50.8	53.7
	Qwen-1.5-7B	56.1	29.8	63.8	54.5	64.2	58.5	49.7	53.8
Qwen-1.5-1.8B	Qwen-1.5-4B	58.7	34.6	67.9	57.7	67.6	64.9	60.7	58.9
	Qwen-1.5-7B	59.3	40.0	68.4	58.7	68.4	65.1	61.5	60.2

## 5 CONCLUSION

In this paper, we introduce LLaVA-MoD, a novel framework for efficient training of small-scale multimodal language models via knowledge distillation from large-scale ones. It addresses two key challenges in MLLM distillation: enhancing s-MLLM architecture with MoE design for efficiency and expressiveness balance and implementing a progressive knowledge transfer strategy. Extensive experiments show that LLaVA-MoD outperforms existing models with low activation parameters and computational costs. Notably, it outperforms Qwen-VL-Chat-7B by 8.8% with only 2 billion activation parameters, 0.3% training data, and 23% trainable parameters, highlighting its effectiveness in distilling knowledge and driving more efficient multimodal language model development.

## 6 LIMITATIONS

LLaVA-MoD requires that both the teacher and student models belong to the same family of large language models (LLMs) to ensure consistency in the vocabulary space. Future research could explore distillation techniques involving heterogeneous model families. Additionally, the need to load both student and teacher models results in significant memory usage. To facilitate more efficient distillation, a feasible solution would be to pre-extract the outputs of the teacher model, allowing only the student model to be loaded during training.

## REFERENCES

- Josh Achiam, Steven Adler, Sandhini Agarwal, Lama Ahmad, Ilge Akkaya, Florencia Leoni Aleman, Diogo Almeida, Janko Altschmidt, Sam Altman, Shyamal Anadkat, et al. Gpt-4 technical report. *arXiv preprint arXiv:2303.08774*, 2023.
- Rishabh Agarwal, Nino Vieillard, Piotr Stanczyk, Sabela Ramos, Matthieu Geist, and Olivier Bachem. GKD: generalized knowledge distillation for auto-regressive sequence models. *CoRR*, abs/2306.13649, 2023. doi: 10.48550/ARXIV.2306.13649. URL <https://doi.org/10.48550/arXiv.2306.13649>.
- Jean-Baptiste Alayrac, Jeff Donahue, Pauline Luc, Antoine Miech, Iain Barr, Yana Hasson, Karel Lenc, Arthur Mensch, Katherine Millican, Malcolm Reynolds, Roman Ring, Eliza Rutherford, Serkan Cabi, Tengda Han, Zhitao Gong, Sina Samangooei, Marianne Monteiro, Jacob L. Menick, Sebastian Borgeaud, Andy Brock, Aida Nematzadeh, Sahand Sharifzadeh, Mikolaj Binkowski, Ricardo Barreira, Oriol Vinyals, Andrew Zisserman, and Karén Simonyan. Flamingo: a visual language model for few-shot learning. In Sanmi Koyejo, S. Mohamed, A. Agarwal, Danielle Belgrave, K. Cho, and A. Oh (eds.), *Advances in Neural Information Processing Systems 35: Annual Conference on Neural Information Processing Systems 2022, NeurIPS 2022, New Orleans, LA, USA, November 28 - December 9, 2022*, 2022. URL [http://papers.nips.cc/paper\\_files/paper/2022/hash/960a172bc7fbf0177cccbb411a7d800-Abstract-Conference.html](http://papers.nips.cc/paper_files/paper/2022/hash/960a172bc7fbf0177cccbb411a7d800-Abstract-Conference.html).
- Anas Awadalla, Le Xue, Oscar Lo, Manli Shu, Hannah Lee, Etash Kumar Guha, Matt Jordan, Sheng Shen, Mohamed Awadalla, Silvio Savarese, et al. Mint-1t: Scaling open-source multimodal data by 10x: A multimodal dataset with one trillion tokens. *arXiv preprint arXiv:2406.11271*, 2024.
- Jinze Bai, Shuai Bai, Yunfei Chu, Zeyu Cui, Kai Dang, Xiaodong Deng, Yang Fan, Wenbin Ge, Yu Han, Fei Huang, Binyuan Hui, Luo Ji, Mei Li, Junyang Lin, Runji Lin, Dayiheng Liu, Gao Liu, Chengqiang Lu, Keming Lu, Jianxin Ma, Rui Men, Xingzhang Ren, Xuancheng Ren, Chuanqi Tan, Sinan Tan, Jianhong Tu, Peng Wang, Shijie Wang, Wei Wang, Shengguang Wu, Benfeng Xu, Jin Xu, An Yang, Hao Yang, Jian Yang, Shusheng Yang, Yang Yao, Bowen Yu, Hongyi Yuan, Zheng Yuan, Jianwei Zhang, Xingxuan Zhang, Yichang Zhang, Zhenru Zhang, Chang Zhou, Jingren Zhou, Xiaohuan Zhou, and Tianhang Zhu. Qwen technical report. *arXiv preprint arXiv:2309.16609*, 2023a.
- Jinze Bai, Shuai Bai, Shusheng Yang, Shijie Wang, Sinan Tan, Peng Wang, Junyang Lin, Chang Zhou, and Jingren Zhou. Qwen-vl: A frontier large vision-language model with versatile abilities. *arXiv preprint arXiv:2308.12966*, 2023b.
- Jie Cao and Jing Xiao. An augmented benchmark dataset for geometric question answering through dual parallel text encoding. In *COLING*, pp. 1511–1520, 2022.
- Mathilde Caron, Hugo Touvron, Ishan Misra, Hervé Jégou, Julien Mairal, Piotr Bojanowski, and Armand Joulin. Emerging properties in self-supervised vision transformers. In *Proceedings of the IEEE/CVF international conference on computer vision*, pp. 9650–9660, 2021.
- Guiming Hardy Chen, Shunian Chen, Ruifei Zhang, Junying Chen, Xiangbo Wu, Zhiyi Zhang, Zhihong Chen, Jianquan Li, Xiang Wan, and Benyou Wang. Allava: Harnessing gpt4v-synthesized data for a lite vision-language model. *arXiv preprint arXiv:2402.11684*, 2024.
- Lin Chen, Jisong Li, Xiaoyi Dong, Pan Zhang, Conghui He, Jiaqi Wang, Feng Zhao, and Dahua Lin. Sharegpt4v: Improving large multi-modal models with better captions. *arXiv preprint arXiv:2311.12793*, 2023a.
- Zhe Chen, Jiannan Wu, Wenhai Wang, Weijie Su, Guo Chen, Sen Xing, Muyan Zhong, Qinglong Zhang, Xizhou Zhu, Lewei Lu, Bin Li, Ping Luo, Tong Lu, Yu Qiao, and Jifeng Dai. Internvl: Scaling up vision foundation models and aligning for generic visual-linguistic tasks. *arXiv preprint arXiv:2312.14238*, 2023b.
- X Chu, L Qiao, X Lin, S Xu, Y Yang, Y Hu, F Wei, X Zhang, B Zhang, X Wei, et al. Mobilevlm: A fast, strong and open vision language assistant for mobile devices. *arXiv preprint arXiv:2312.16886*, 2023.

- Xiangxiang Chu, Limeng Qiao, Xinyu Zhang, Shuang Xu, Fei Wei, Yang Yang, Xiaofei Sun, Yiming Hu, Xinyang Lin, Bo Zhang, et al. MobileVLM v2: Faster and stronger baseline for vision language model. *arXiv preprint arXiv:2402.03766*, 2024.
- Christopher Clark and Matt Gardner. Simple and effective multi-paragraph reading comprehension. In *ACL*, pp. 845–855, 2018.
- Damai Dai, Chengqi Deng, Chenggang Zhao, RX Xu, Huazuo Gao, Deli Chen, Jiashi Li, Wangding Zeng, Xingkai Yu, Y Wu, et al. Deepseekmoe: Towards ultimate expert specialization in mixture-of-experts language models. *arXiv preprint arXiv:2401.06066*, 2024.
- P Kingma Diederik. Adam: A method for stochastic optimization. (*No Title*), 2014.
- Abhimanyu Dubey, Abhinav Jauhri, Abhinav Pandey, Abhishek Kadian, Ahmad Al-Dahle, Aiesha Letman, Akhil Mathur, Alan Schelten, Amy Yang, Angela Fan, et al. The llama 3 herd of models. *arXiv preprint arXiv:2407.21783*, 2024.
- Lijie Fan, Dilip Krishnan, Phillip Isola, Dina Katabi, and Yonglong Tian. Improving clip training with language rewrites. *Advances in Neural Information Processing Systems*, 36, 2024.
- William Fedus, Barret Zoph, and Noam Shazeer. Switch transformers: Scaling to trillion parameter models with simple and efficient sparsity. *Journal of Machine Learning Research*, 23(120):1–39, 2022.
- Chaoyou Fu, Peixian Chen, Yunhang Shen, Yulei Qin, Mengdan Zhang, Xu Lin, Jinrui Yang, Xiawu Zheng, Ke Li, Xing Sun, et al. MME: A comprehensive evaluation benchmark for multimodal large language models. *arXiv preprint arXiv:2306.13394*, 2023.
- Samir Yitzhak Gadre, Gabriel Ilharco, Alex Fang, Jonathan Hayase, Georgios Smyrnis, Thao Nguyen, Ryan Marten, Mitchell Wortsman, Dhruva Ghosh, Jieyu Zhang, et al. Datacomp: In search of the next generation of multimodal datasets. *Advances in Neural Information Processing Systems*, 36, 2024.
- Peng Gao, Renrui Zhang, Chris Liu, Longtian Qiu, Siyuan Huang, Weifeng Lin, Shitian Zhao, Shijie Geng, Ziyi Lin, Peng Jin, et al. Sphinx-x: Scaling data and parameters for a family of multi-modal large language models. *arXiv preprint arXiv:2402.05935*, 2024.
- Yash Goyal, Tejas Khot, Douglas Summers-Stay, Dhruv Batra, and Devi Parikh. Making the v in vqa matter: Elevating the role of image understanding in visual question answering. In *CVPR*, pp. 6904–6913, 2017.
- Yuxian Gu, Li Dong, Furu Wei, and Minlie Huang. Minillm: Knowledge distillation of large language models. In *The Twelfth International Conference on Learning Representations*, 2023.
- Danna Gurari, Qing Li, Abigale J Stangl, Anhong Guo, Chi Lin, Kristen Grauman, Jiebo Luo, and Jeffrey P Bigham. Vizwiz grand challenge: Answering visual questions from blind people. In *Proceedings of the IEEE conference on computer vision and pattern recognition*, pp. 3608–3617, 2018.
- Muyang He, Yexin Liu, Boya Wu, Jianhao Yuan, Yueze Wang, Tiejun Huang, and Bo Zhao. Efficient multimodal learning from data-centric perspective. *arXiv preprint arXiv:2402.11530*, 2024.
- Geoffrey Hinton, Oriol Vinyals, and Jeff Dean. Distilling the knowledge in a neural network. *arXiv preprint arXiv:1503.02531*, 2015.
- Namgyu Ho, Laura Schmid, and Se-Young Yun. Large language models are reasoning teachers. In Anna Rogers, Jordan L. Boyd-Graber, and Naoaki Okazaki (eds.), *Proceedings of the 61st Annual Meeting of the Association for Computational Linguistics (Volume 1: Long Papers)*, *ACL 2023, Toronto, Canada, July 9-14, 2023*, pp. 14852–14882. Association for Computational Linguistics, 2023. doi: 10.18653/V1/2023.ACL-LONG.830. URL <https://doi.org/10.18653/v1/2023.acl-long.830>.

- Qidong Huang, Xiaoyi Dong, Pan Zhang, Bin Wang, Conghui He, Jiaqi Wang, Dahua Lin, Weiming Zhang, and Nenghai Yu. Opera: Alleviating hallucination in multi-modal large language models via over-trust penalty and retrospection-allocation. In *Proceedings of the IEEE/CVF Conference on Computer Vision and Pattern Recognition*, pp. 13418–13427, 2024.
- Yukun Huang, Yanda Chen, Zhou Yu, and Kathleen R. McKeown. In-context learning distillation: Transferring few-shot learning ability of pre-trained language models. *CoRR*, abs/2212.10670, 2022. doi: 10.48550/ARXIV.2212.10670. URL <https://doi.org/10.48550/arXiv.2212.10670>.
- Drew A Hudson and Christopher D Manning. Gqa: A new dataset for real-world visual reasoning and compositional question answering. In *Proceedings of the IEEE/CVF conference on computer vision and pattern recognition*, pp. 6700–6709, 2019.
- Robert A. Jacobs, Michael I. Jordan, Steven J. Nowlan, and Geoffrey E. Hinton. Adaptive mixtures of local experts. *Neural Computation*, 3(1):79–87, 1991. doi: 10.1162/neco.1991.3.1.79.
- Albert Q. Jiang, Alexandre Sablayrolles, Antoine Roux, Arthur Mensch, Blanche Savary, Chris Bamford, Devendra Singh Chaplot, Diego de las Casas, Emma Bou Hanna, Florian Bressand, Gianna Lengyel, Guillaume Bour, Guillaume Lample, L  lio Renard Lavaud, Lucile Saulnier, Marie-Anne Lachaux, Pierre Stock, Sandeep Subramanian, Sophia Yang, Szymon Antoniak, Teven Le Scao, Th  ophile Gerv  t, Thibaut Lavril, Thomas Wang, Timoth  e Lacroix, and William El Sayed. Mixtral of experts, 2024. URL <https://arxiv.org/abs/2401.04088>.
- Kushal Kafle, Brian Price, Scott Cohen, and Christopher Kanan. Dvqa: Understanding data visualizations via question answering. In *CVPR*, pp. 5648–5656, 2018.
- Aniruddha Kembhavi, Mike Salvato, Eric Kolve, Minjoon Seo, Hannaneh Hajishirzi, and Ali Farhadi. A diagram is worth a dozen images. In *ECCV*, pp. 235–251, 2016.
- Geewook Kim, Teakgyu Hong, Moonbin Yim, JeongYeon Nam, Jinyoung Park, Jinyeong Yim, Wonseok Hwang, Sangdoo Yun, Dongyoon Han, and Seunghyun Park. Ocr-free document understanding transformer. In *ECCV*, 2022.
- Aran Komatsuzaki, Joan Puigcerver, James Lee-Thorp, Carlos Riquelme Ruiz, Basil Mustafa, Joshua Ainslie, Yi Tay, Mostafa Dehghani, and Neil Houlsby. Sparse upcycling: Training mixture-of-experts from dense checkpoints. *arXiv preprint arXiv:2212.05055*, 2022.
- Ranjay Krishna, Yuke Zhu, Oliver Groth, Justin Johnson, Kenji Hata, Joshua Kravitz, Stephanie Chen, Yannis Kalantidis, Li-Jia Li, David A Shamma, et al. Visual genome: Connecting language and vision using crowdsourced dense image annotations. *IJCV*, 123:32–73, 2017.
- Sicong Leng, Hang Zhang, Guanzheng Chen, Xin Li, Shijian Lu, Chunyan Miao, and Lidong Bing. Mitigating object hallucinations in large vision-language models through visual contrastive decoding. In *Proceedings of the IEEE/CVF Conference on Computer Vision and Pattern Recognition*, pp. 13872–13882, 2024.
- Dmitry Lepikhin, HyoukJoong Lee, Yuanzhong Xu, Dehao Chen, Orhan Firat, Yanping Huang, Maxim Krikun, Noam Shazeer, and Zhifeng Chen. Gshard: Scaling giant models with conditional computation and automatic sharding, 2020. URL <https://arxiv.org/abs/2006.16668>.
- Bo Li, Yuanhan Zhang, Liangyu Chen, Jinghao Wang, Fanyi Pu, Jingkang Yang, Chunyuan Li, and Ziwei Liu. Mimic-it: Multi-modal in-context instruction tuning. *arXiv preprint arXiv:2306.05425*, 2023a.
- Bo Li, Kaichen Zhang, Hao Zhang, Dong Guo, Renrui Zhang, Feng Li, Yuanhan Zhang, Ziwei Liu, and Chunyuan Li. Llava-next: Stronger llms supercharge multimodal capabilities in the wild, May 2024a. URL <https://llava-vl.github.io/blog/2024-05-10-llava-next-stronger-llms/>.

- Junnan Li, Dongxu Li, Silvio Savarese, and Steven C. H. Hoi. BLIP-2: bootstrapping language-image pre-training with frozen image encoders and large language models. In Andreas Krause, Emma Brunskill, Kyunghyun Cho, Barbara Engelhardt, Sivan Sabato, and Jonathan Scarlett (eds.), *International Conference on Machine Learning, ICML 2023, 23-29 July 2023, Honolulu, Hawaii, USA*, volume 202 of *Proceedings of Machine Learning Research*, pp. 19730–19742. PMLR, 2023b. URL <https://proceedings.mlr.press/v202/li23q.html>.
- Shiyang Li, Jianshu Chen, Yelong Shen, Zhiyu Chen, Xinlu Zhang, Zekun Li, Hong Wang, Jing Qian, Baolin Peng, Yi Mao, Wenhui Chen, and Xifeng Yan. Explanations from large language models make small reasoners better. *CoRR*, abs/2210.06726, 2022. doi: 10.48550/ARXIV.2210.06726. URL <https://doi.org/10.48550/arXiv.2210.06726>.
- Xianhang Li, Haoqin Tu, Mude Hui, Zeyu Wang, Bingchen Zhao, Junfei Xiao, Sucheng Ren, Jieru Mei, Qing Liu, Huangjie Zheng, et al. What if we recaption billions of web images with llama-3? *arXiv preprint arXiv:2406.08478*, 2024b.
- Yanwei Li, Yuechen Zhang, Chengyao Wang, Zhisheng Zhong, Yixin Chen, Ruihang Chu, Shaoteng Liu, and Jiaya Jia. Mini-gemini: Mining the potential of multi-modality vision language models. *CoRR*, abs/2403.18814, 2024c. doi: 10.48550/ARXIV.2403.18814. URL <https://doi.org/10.48550/arXiv.2403.18814>.
- Yifan Li, Yifan Du, Kun Zhou, Jinpeng Wang, Wayne Xin Zhao, and Ji-Rong Wen. Evaluating object hallucination in large vision-language models. *arXiv preprint arXiv:2305.10355*, 2023c.
- Bin Lin, Zhenyu Tang, Yang Ye, Jiaxi Cui, Bin Zhu, Peng Jin, Junwu Zhang, Munan Ning, and Li Yuan. Moe-llava: Mixture of experts for large vision-language models. *arXiv preprint arXiv:2401.15947*, 2024a.
- Ji Lin, Hongxu Yin, Wei Ping, Pavlo Molchanov, Mohammad Shoeybi, and Song Han. Vila: On pre-training for visual language models. In *Proceedings of the IEEE/CVF Conference on Computer Vision and Pattern Recognition*, pp. 26689–26699, 2024b.
- Fuxiao Liu, Kevin Lin, Linjie Li, Jianfeng Wang, Yaser Yacoob, and Lijuan Wang. Aligning large multi-modal model with robust instruction tuning. *arXiv preprint arXiv:2306.14565*, 2023a.
- Haotian Liu, Chunyuan Li, Yuheng Li, and Yong Jae Lee. Improved baselines with visual instruction tuning. *arXiv preprint arXiv:2310.03744*, 2023b.
- Haotian Liu, Chunyuan Li, Qingyang Wu, and Yong Jae Lee. Visual instruction tuning. *Advances in neural information processing systems*, 36, 2024.
- Yuan Liu, Haodong Duan, Yuanhan Zhang, Bo Li, Songyang Zhang, Wangbo Zhao, Yike Yuan, Jiaqi Wang, Conghui He, Ziwei Liu, et al. Mmbench: Is your multi-modal model an all-around player? *arXiv preprint arXiv:2307.06281*, 2023c.
- Zhuang Liu, Hanzi Mao, Chao-Yuan Wu, Christoph Feichtenhofer, Trevor Darrell, and Saining Xie. A convnet for the 2020s. In *Proceedings of the IEEE/CVF conference on computer vision and pattern recognition*, pp. 11976–11986, 2022.
- Haoyu Lu, Wen Liu, Bo Zhang, Bingxuan Wang, Kai Dong, Bo Liu, Jingxiang Sun, Tongzheng Ren, Zhuoshu Li, Yaofeng Sun, et al. Deepseek-vl: towards real-world vision-language understanding. *arXiv preprint arXiv:2403.05525*, 2024.
- Pan Lu, Swaroop Mishra, Tanglin Xia, Liang Qiu, Kai-Wei Chang, Song-Chun Zhu, Oyvind Tafjord, Peter Clark, and Ashwin Kalyan. Learn to explain: Multimodal reasoning via thought chains for science question answering. *NeurIPS*, 35:2507–2521, 2022a.
- Pan Lu, Swaroop Mishra, Tony Xia, Liang Qiu, Kai-Wei Chang, Song-Chun Zhu, Oyvind Tafjord, Peter Clark, and Ashwin Kalyan. Learn to explain: Multimodal reasoning via thought chains for science question answering. In *The 36th Conference on Neural Information Processing Systems (NeurIPS)*, 2022b.
- Junhua Mao, Jonathan Huang, Alexander Toshev, Oana Camburu, Alan L Yuille, and Kevin Murphy. Generation and comprehension of unambiguous object descriptions. In *CVPR*, pp. 11–20, 2016.



- Kenneth Marino, Mohammad Rastegari, Ali Farhadi, and Roozbeh Mottaghi. Ok-vqa: A visual question answering benchmark requiring external knowledge. In *CVPR*, pp. 3195–3204, 2019.
- Ahmed Masry, Xuan Long Do, Jia Qing Tan, Shafiq Joty, and Enamul Hoque. Chartqa: A benchmark for question answering about charts with visual and logical reasoning. In *ACL*, pp. 2263–2279, 2022.
- Anand Mishra, Shashank Shekhar, Ajeet Kumar Singh, and Anirban Chakraborty. Ocr-vqa: Visual question answering by reading text in images. In *ICDAR*, pp. 947–952, 2019.
- Subhabrata Mukherjee, Arindam Mitra, Ganesh Jawahar, Sahaj Agarwal, Hamid Palangi, and Ahmed Awadallah. Orca: Progressive learning from complex explanation traces of GPT-4. *CoRR*, abs/2306.02707, 2023. doi: 10.48550/ARXIV.2306.02707. URL <https://doi.org/10.48550/arXiv.2306.02707>.
- Thao Nguyen, Samir Yitzhak Gadre, Gabriel Ilharco, Sewoong Oh, and Ludwig Schmidt. Improving multimodal datasets with image captioning. *Advances in Neural Information Processing Systems*, 36, 2024.
- Alec Radford, Jong Wook Kim, Chris Hallacy, Aditya Ramesh, Gabriel Goh, Sandhini Agarwal, Girish Sastry, Amanda Askell, Pamela Mishkin, Jack Clark, et al. Learning transferable visual models from natural language supervision. In *International conference on machine learning*, pp. 8748–8763. PMLR, 2021.
- Rafael Rafailov, Archit Sharma, Eric Mitchell, Christopher D Manning, Stefano Ermon, and Chelsea Finn. Direct preference optimization: Your language model is secretly a reward model. *Advances in Neural Information Processing Systems*, 36, 2024.
- Christoph Schuhmann, Richard Vencu, Romain Beaumont, Robert Kaczmarczyk, Clayton Mullis, Aarush Katta, Theo Coombes, Jenia Jitsev, and Aran Komatsuzaki. Laion-400m: Open dataset of clip-filtered 400 million image-text pairs. *arXiv preprint arXiv:2111.02114*, 2021.
- Christoph Schuhmann, Romain Beaumont, Richard Vencu, Cade Gordon, Ross Wightman, Mehdi Cherti, Theo Coombes, Aarush Katta, Clayton Mullis, Mitchell Wortsman, et al. Laion-5b: An open large-scale dataset for training next generation image-text models. *Advances in Neural Information Processing Systems*, 35:25278–25294, 2022.
- Dustin Schwenk, Apoorv Khandelwal, Christopher Clark, Kenneth Marino, and Roozbeh Mottaghi. A-okvqa: A benchmark for visual question answering using world knowledge. In *ECCV*, pp. 146–162, 2022.
- Zhenwei Shao, Zhou Yu, Jun Yu, Xuecheng Ouyang, Lihao Zheng, Zhenbiao Gai, Mingyang Wang, and Jiajun Ding. Imp: Highly capable large multimodal models for mobile devices. *arXiv preprint arXiv:2405.12107*, 2024.
- Sheng Shen, Zhewei Yao, Chunyuan Li, Trevor Darrell, Kurt Keutzer, and Yuxiong He. Scaling vision-language models with sparse mixture of experts. *arXiv preprint arXiv:2303.07226*, 2023.
- Fangxun Shu, Lei Zhang, Hao Jiang, and Cihang Xie. Audio-visual llm for video understanding. *arXiv preprint arXiv:2312.06720*, 2023.
- Oleksii Sidorov, Ronghang Hu, Marcus Rohrbach, and Amanpreet Singh. Textcaps: a dataset for image captioning with reading comprehension. In *ECCV*, pp. 742–758, 2020.
- Amanpreet Singh, Vivek Natarajan, Meet Shah, Yu Jiang, Xinlei Chen, Dhruv Batra, Devi Parikh, and Marcus Rohrbach. Towards vqa models that can read. In *Proceedings of the IEEE/CVF conference on computer vision and pattern recognition*, pp. 8317–8326, 2019.
- Zhiqing Sun, Sheng Shen, Shengcao Cao, Haotian Liu, Chunyuan Li, Yikang Shen, Chuang Gan, Liang-Yan Gui, Yu-Xiong Wang, Yiming Yang, et al. Aligning large multimodal models with factually augmented rlhf. *arXiv preprint arXiv:2309.14525*, 2023.

- Gemini Team, Rohan Anil, Sebastian Borgeaud, Yonghui Wu, Jean-Baptiste Alayrac, Jiahui Yu, Radu Soricut, Johan Schalkwyk, Andrew M Dai, Anja Hauth, et al. Gemini: a family of highly capable multimodal models. *arXiv preprint arXiv:2312.11805*, 2023.
- Hugo Touvron, Thibaut Lavril, Gautier Izacard, Xavier Martinet, Marie-Anne Lachaux, Timothée Lacroix, Baptiste Rozière, Naman Goyal, Eric Hambro, Faisal Azhar, et al. Llama: Open and efficient foundation language models. *arXiv preprint arXiv:2302.13971*, 2023a.
- Hugo Touvron, Louis Martin, Kevin Stone, Peter Albert, Amjad Almahairi, Yasmine Babaei, Nikolay Bashlykov, Soumya Batra, Prajjwal Bhargava, Shruti Bhosale, et al. Llama 2: Open foundation and fine-tuned chat models. *arXiv preprint arXiv:2307.09288*, 2023b.
- Junke Wang, Lingchen Meng, Zejia Weng, Bo He, Zuxuan Wu, and Yu-Gang Jiang. To see is to believe: Prompting gpt-4v for better visual instruction tuning. *arXiv preprint arXiv:2311.07574*, 2023a.
- Junyang Wang, Yuhang Wang, Guohai Xu, Jing Zhang, Yukai Gu, Haitao Jia, Ming Yan, Ji Zhang, and Jitao Sang. An llm-free multi-dimensional benchmark for mllms hallucination evaluation. *arXiv preprint arXiv:2311.07397*, 2023b.
- Wenhai Wang, Zhe Chen, Xiaokang Chen, Jiannan Wu, Xizhou Zhu, Gang Zeng, Ping Luo, Tong Lu, Jie Zhou, Yu Qiao, and Jifeng Dai. Visionllm: Large language model is also an open-ended decoder for vision-centric tasks. In Alice Oh, Tristan Naumann, Amir Globerson, Kate Saenko, Moritz Hardt, and Sergey Levine (eds.), *Advances in Neural Information Processing Systems 36: Annual Conference on Neural Information Processing Systems 2023, NeurIPS 2023, New Orleans, LA, USA, December 10 - 16, 2023*, 2023c. URL [http://papers.nips.cc/paper\\_files/paper/2023/hash/c1f7b1ed763e9c75e4db74b49b76db5f-Abstract-Conference.html](http://papers.nips.cc/paper_files/paper/2023/hash/c1f7b1ed763e9c75e4db74b49b76db5f-Abstract-Conference.html).
- Hu Xu, Saining Xie, Po-Yao Huang, Licheng Yu, Russell Howes, Gargi Ghosh, Luke Zettlemoyer, and Christoph Feichtenhofer. Cit: Curation in training for effective vision-language data. In *Proceedings of the IEEE/CVF International Conference on Computer Vision*, pp. 15180–15189, 2023.
- An Yang, Baosong Yang, Binyuan Hui, Bo Zheng, Bowen Yu, Chang Zhou, Chengpeng Li, Chengyuan Li, Dayiheng Liu, Fei Huang, et al. Qwen2 technical report. *arXiv preprint arXiv:2407.10671*, 2024.
- Yuan Yao, Tianyu Yu, Ao Zhang, Chongyi Wang, Junbo Cui, Hongji Zhu, Tianchi Cai, Haoyu Li, Weilin Zhao, Zhihui He, et al. Minicpm-v: A gpt-4v level mllm on your phone. *arXiv preprint arXiv:2408.01800*, 2024.
- Licheng Yu, Patrick Poirson, Shan Yang, Alexander C Berg, and Tamara L Berg. Modeling context in referring expressions. In *ECCV*, pp. 69–85, 2016.
- Tianyu Yu, Yuan Yao, Haoye Zhang, Taiwen He, Yifeng Han, Ganqu Cui, Jinyi Hu, Zhiyuan Liu, Hai-Tao Zheng, Maosong Sun, et al. Rlhf-v: Towards trustworthy mllms via behavior alignment from fine-grained correctional human feedback. In *Proceedings of the IEEE/CVF Conference on Computer Vision and Pattern Recognition*, pp. 13807–13816, 2024a.
- Tianyu Yu, Haoye Zhang, Yuan Yao, Yunkai Dang, Da Chen, Xiaoman Lu, Ganqu Cui, Taiwen He, Zhiyuan Liu, Tat-Seng Chua, et al. Rlaif-v: Aligning mllms through open-source ai feedback for super gpt-4v trustworthiness. *arXiv preprint arXiv:2405.17220*, 2024b.
- Zhengqing Yuan, Zhaoxu Li, and Lichao Sun. Tinygpt-v: Efficient multimodal large language model via small backbones. *arXiv preprint arXiv:2312.16862*, 2023.
- Lei Zhang, Fangxun Shu, Sucheng Ren, Bingchen Zhao, Hao Jiang, and Cihang Xie. Compress & align: Curating image-text data with human knowledge. *arXiv preprint arXiv:2312.06726*, 2023.
- Bo Zhao, Boya Wu, and Tiejun Huang. Svit: Scaling up visual instruction tuning. *arXiv preprint arXiv:2307.04087*, 2023a.

- Zhiyuan Zhao, Bin Wang, Linke Ouyang, Xiaoyi Dong, Jiaqi Wang, and Conghui He. Beyond hallucinations: Enhancing lvlms through hallucination-aware direct preference optimization. *arXiv preprint arXiv:2311.16839*, 2023b.
- Baichuan Zhou, Ying Hu, Xi Weng, Junlong Jia, Jie Luo, Xien Liu, Ji Wu, and Lei Huang. Tinyllava: A framework of small-scale large multimodal models. *arXiv preprint arXiv:2402.14289*, 2024a.
- Yiyang Zhou, Chenhang Cui, Jaehong Yoon, Linjun Zhang, Zhun Deng, Chelsea Finn, Mohit Bansal, and Huaxiu Yao. Analyzing and mitigating object hallucination in large vision-language models. *arXiv preprint arXiv:2310.00754*, 2023.
- Yiyang Zhou, Chenhang Cui, Rafael Rafailov, Chelsea Finn, and Huaxiu Yao. Aligning modalities in vision large language models via preference fine-tuning. *arXiv preprint arXiv:2402.11411*, 2024b.
- Deyao Zhu, Jun Chen, Xiaoqian Shen, Xiang Li, and Mohamed Elhoseiny. Minigpt-4: Enhancing vision-language understanding with advanced large language models. *CoRR*, abs/2304.10592, 2023. doi: 10.48550/ARXIV.2304.10592. URL <https://doi.org/10.48550/arXiv.2304.10592>.
- Wanrong Zhu, Jack Hessel, Anas Awadalla, Samir Yitzhak Gadre, Jesse Dodge, Alex Fang, Youngjae Yu, Ludwig Schmidt, William Yang Wang, and Yejin Choi. Multimodal c4: An open, billion-scale corpus of images interleaved with text. *Advances in Neural Information Processing Systems*, 36, 2024.

## A APPENDIX

### A.1 DATASET

We report the detailed training dataset settings of LLaVA-MoD in Table A.1.

Table 10: Training dataset. **#Sample** means the training samples.

Stage	Task	Dataset
Initialization	Captioning	LLaVA-1.5-Pretrain (Liu et al., 2023b)
Dense-to-Dense Distillation	Captioning	ALLaVA-Caption-4V (Chen et al., 2024), ShareGPT4V-PT (Chen et al., 2023a)
	Conversation	MIMIC-IT (Li et al., 2023a), LVIS (Wang et al., 2023a), LRV (Liu et al., 2023a), SViT (Zhao et al., 2023a)
Dense-to-Sparse Distillation	Captioning	ShareGPT4V-100K (Chen et al., 2023a), TextCaps (Sidorov et al., 2020)
	Conversation	LLaVA-1.5-Instruct (Liu et al., 2023b)
	General QA	GQA (Hudson & Manning, 2019), VQAv2 (Goyal et al., 2017), OKVQA (Marino et al., 2019)
	Grounding	Visual Genome (Krishna et al., 2017), RefCOCO (Yu et al., 2016; Mao et al., 2016)
	Science	AI2D (Kembhavi et al., 2016), ScienceQA (Lu et al., 2022a)
	Chart & Doc	DVQA (Kafle et al., 2018), ChartQA (Masry et al., 2022), DocQA (Clark & Gardner, 2018)
	OCR	OCRVQA (Mishra et al., 2019), SynthDoG-EN (Kim et al., 2022)
	Knowledge	A-OKVQA (Schwenk et al., 2022), GeoQA+ (Cao & Xiao, 2022)
Preference Distillation	Preference	RLAIF-V (Yu et al., 2024b)

### A.2 HYPERPARAMETERS

We report the detailed training hyperparameters of LLaVA-MoD in Table A.2.

Table 11: Training hyperparameters

Configuration	Stage-1	Stage-2	Stage-3
LLM	✗	✓	✓
VL Adaptor	✓	✓	✓
ViT	✗	✗	✗
LLM init.	Qwen-1.5-1.8B	Qwen-1.5-1.8B	2nd-stage
VL Adaptor init.	MLP	1st-stage	2nd-stage
ViT init.		CLIP-Large@336	
Image resolution		336 × 336	
ViT sequence length		576	
LLM sequence length		2048	
Optimizer		AdamW	
Optimizer hyperparameter	$\beta_1 = 0.9, \beta_2 = 0.98, eps = 1e^{-6}$	$2e^{-5}$	$2e^{-5}$
Learning rate	$1e^{-4}$		
Learning rate schedule		Cosine decay	
Weight decay		0.0	
Training epoch		1	
Warm-up ratio		0.03	
Global batch size	256	128	128
Numerical precision		Bfloat16	
Model parallelism	Zero2	Zero2 offload	Zero2 offload